ISBN: 978-3-95450-229-5 ISSN: 2673-5520 doi:10.18429/JACoW-MEDSI2020-MOPC10

MECHANICAL DESIGN PROGRESS OF THE IN SITU NANOPROBE INSTRUMENT FOR APS-U*

Steven P. Kearney†, Deming Shu, Tim Mooney, Barry Lai, Si Chen, and Jörg Maser
Advanced Photon Source, Argonne National Laboratory, Lemont, IL 60439, U.S.A.

Abstract

The In Situ Nanoprobe (ISN, 19-ID) beamline will be a new best-in-class long beamline to be constructed as part of the Advanced Photon Source Upgrade (APS-U) project [1, 2]. To achieve long working distance at high spatial resolution, the ISN instrument will be positioned 210 m downstream of the x-ray source, in a dedicated satellite building, currently under construction [3]. The ISN instrument will use a nano-focusing Kirkpatrick-Baez (K-B) mirror system, which will focus hard x-rays to a focal spot as small as 20 nm, with a large working distance of 61 mm. The large working distance provides space for various *in situ* sample cells for x-ray fluorescence tomography and ptychographic 3D imaging, allows the use of a separate, independent vacuum chambers for the optics and sample, and provides the flexibility to run experiments in vacuum or at ambient pressure. A consequence of the small spot size and large working distance are stringent requirements for high angular stability of the K-B mirrors (5 nrad V-mirror and 16 nrad H-mirror) and high relative stability between focus spot and sample (4 nm_{RMS}). Additional features include fly-scanning up to 2 kg mass, sample plus *in situ* cell, at 1 mm/s in vertical and/or horizontal directions over an area of 10 mm x 10 mm. Environmental capabilities will include heating and cooling, flow of fluids and applied fields, as required for electrochemistry and flow of gases at high temperature for catalysis. To achieve these capabilities and precise requirements we have used precision engineering fundamentals to guide the design process.

INTRODUCTION

The advanced photon source (APS) at Argonne National Laboratory (ANL) is being upgraded with a new multi-bend achromat storage ring lattice and insertion devices that will provide increased brightness and coherence through reduced emittance of the stored electron beam [4]. To take full advantage of the new beam specifications, a new best-in-class In Situ Nanoprobe (ISN) instrument is being developed for the 19-ID beamline.

The ISN instrument will use a nano-focusing Kirkpatrick-Baez (K-B) mirror system to focus hard x-rays to a focal spot as small as 20 nm, with a large working distance of 61 mm. The large working distance provides space for various *in situ* sample cells for x-ray fluorescence tomography and ptychographic 3D imaging, allows the use of separate, independent vacuum chambers for the optics and sample, and provides the flexibility to run experiments in vacuum or at ambient pressure.

Requirements of the ISN instrument that make it unique and a technically challenging design and allow it to support a broad range of *in situ* conditions are: high angular stability of the K-B mirrors (5 nrad V-mirror and 16 nrad H-mirror) and high relative stability between focus spot and sample (4 nm_{RMS}), fly-scanning a maximum of a 2 kg *in situ* cell at 1 mm/s in vertical and/or horizontal directions over an area of 10 mm x 10 mm, and separate vacuum chambers result in a metrology frame that needs to be transferred between two environments.

Achieving the requirements of ISN has required precision engineering of the entire instrument system from the soil up. All the components of the system need to work together, and any one component could push the instrument out of specification. In this paper we will discuss the design and state of the soil and foundation, enclosure environment, nanopositioning systems, and stable metrology frames. For details on the instrument support, which is a modification of granite stages developed by APS, see Preissner *et al*. [5].

INSTRUMENT DESIGN

Location

The ISN instrument will be positioned 210 m downstream of the x-ray source, in a dedicated satellite building, currently under construction. A sketch of the location of the new satellite building with respect to the main APS building and building schematic of the instrument control room and enclosure floor is shown in Fig. 1.

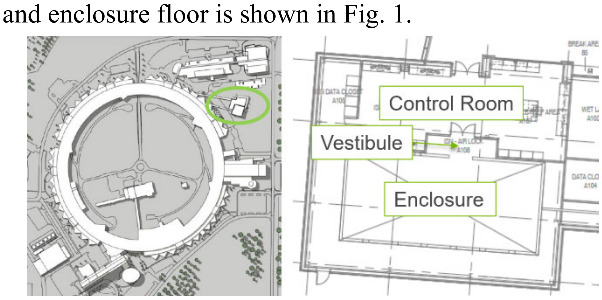

Figure 1: Left, circle is satellite building for ISN and High-Energy X-ray Microscope instruments. Right, floor plan of ISN showing control room, vestibule, and enclosure.

Foundation

We started the design process of the ISN with details of the foundation, which eventually included the soil underneath. To achieve a highly stable floor we measured the vibrations of other similar instrument foundations [3], and found a common successful strategy using slab isolation and 1 m thickness. With an isolated slab, there is a risk of

* This research used resources of the Advanced Photon Source, a U.S. Department of Energy (DOE) Office of Science User Facility at Argonne National Laboratory and is based on research supported by the U.S. DOE Office of Science-Basic Energy Sciences, under Contract No. DE-AC02-06CH11357.
†skearney@anl.gov

ISBN: 978-3-95450-229-5 ISSN: 2673-5520 doi:10.18429/JACoW-MEDSI2020-MOPC10

having too little mass and amplifying frequencies below 10 Hz, therefore we decided on a 1 m thick slab. Going further, we investigated whether the concrete enclosure should be placed on or off the isolated slab. Using lumped parameter models from soil dynamics that describe slab-on-grade vibrations [6], it was found that the added mass of the enclosure decreased the compliance in the vertical direction through increased coupling with the soil, and that it lowered the first natural frequency from 5 Hz to 3 Hz for vertical modes, with negligible impacts on tilt modes [7]. The soil in the calculations was assumed to be engineered fill, which was the replacement of the natural soil based on recommendations from the soil bore analysis.

Enclosure

Thermal stability is a major concern for the stability of the instrument. To deal with thermal drifts we have adopted a 2-stage thermal isolation method plus a separate requirement for the instrument surface temperature. Stage 1 is the control room (see Fig. 1) and is under the control of the main building HVAC system. It acts as the thermal barrier between the outside walls and the enclosure walls. Stage 2 is the instrument enclosure itself, which has two advantages for precise thermal stability. First, it is 12 in thick concrete and has a conductance of 5 W/K through a meter squared section of wall compared to 1791 W/K for our typical steel-lead-steel enclosure walls. For the concrete walls there is much less heat transfer for the same temperature difference compared to metal walls. Second, we will install a dedicated HVAC system for the instrument enclosure that uses low velocity duct socks to distribute laminar air flow evenly and control the air temperature to ±0.05 °C for 1 hr. The final instrument surface temperature requirement, which is the most important as this is what causes the thermal drift, will be controlled to ±0.01 °C for 1 hr.

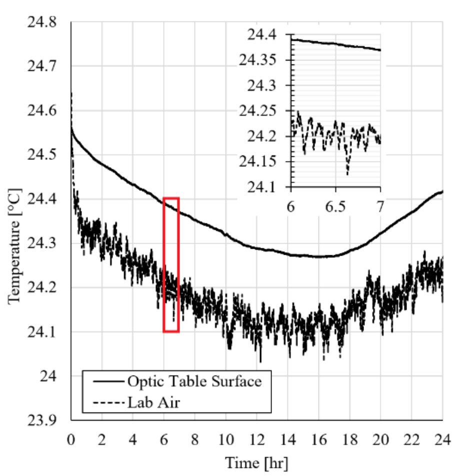

Figure 2: Comparison of air and surface temperatures over 24 hr, acquired with Omega^{TM} precision thermistors.

Cooling using radiant water-cooled panels was implemented at Diamond Light Source and described by Cacho-Nerin *et al*. [8] achieved a 0.017 °C standard deviation stability over a longer period than our one-hour specification. However, we chose a conventional forced air system to avoid cooling pumps and water flow. In addition, a significant gain in stability due to the slow response of thermal masses is expected. An example of this is shown in Fig. 2, where the air temperature and surface temperature of an optics table in lab L1119 at APS was measured. In the inset, the pk-pk surface temperature is 6.5X less than the air.

Vacuum Chambers

Separate vacuum chambers will be used for the K-B optics and sample. The optics chamber will be at UHV pressures, while the sample chamber will be at HV pressures. Separating the environments helps to protect K-B mirror surface and maintain alignment by avoiding pressure cycles to atmosphere during sample changes. This method presents some difficulties in design, such as tight tolerances in assembly, extra windows, and the metrology frame. Accessibility, variability, and shorter sample change time outweighs these added difficulties. Figure 3 shows a cross-sectional view of the two chambers. Gaps between flanges are as small as 2 mm, and there are 2 additional x-ray windows needed to pass through two chamber walls.

The sample chamber is designed to operate with environments of both vacuum and at atmospheric pressure. In vacuum, the sample space available between the chamber wall and focus spot is 47 mm and increases to 55 mm when the top of the sample chamber is removed. Removing the top of the sample chamber is a delicate procedure because of the close tolerances, therefore special jigs and guides are being designed to make this process easier.

Various ports for detectors, sample access, cryostat, and windows can be seen in Fig. 4. Two ports are for SDD fluorescence detectors oriented at 15° and 0° from X. The port at 0° is for a back-scattering geometry detector, and the 15° port is being designed for a multi-element detector and to also accommodate a larger diameter confocal detector. The cryostat port is designed to come from above and slightly off-center from the sample to allow for a clear direct overhead port, which will be for optical or microscope access. Included are ports looking directly at the sample from the horizontal and sample access.

Figure 4 inset shows the details of the combined diffraction window and ptychography window. They are mounted together on the same hinged flange that can be opened for sample access. The flange is curved and will be sealed to the chamber flange using an o-ring seal held in a dovetail cut to keep it in place. The Be window gives a diffraction cone of 7°-60° in the vertical and -5°-60° in the horizontal and has a radius of 120 mm. Ideally, the Be window will be 0.5 mm thick, which does hold vacuum without breaking, however, from and operations point of view, it is risky for the window to be so thin. So, the thickness is still being optimized. The ptychography window will be Si_3N_4 and its dimensions are still be optimized as well.

ISBN: 978-3-95450-229-5 ISSN: 2673-5520 doi:10.18429/JACoW-MEDSI2020-MOPC10

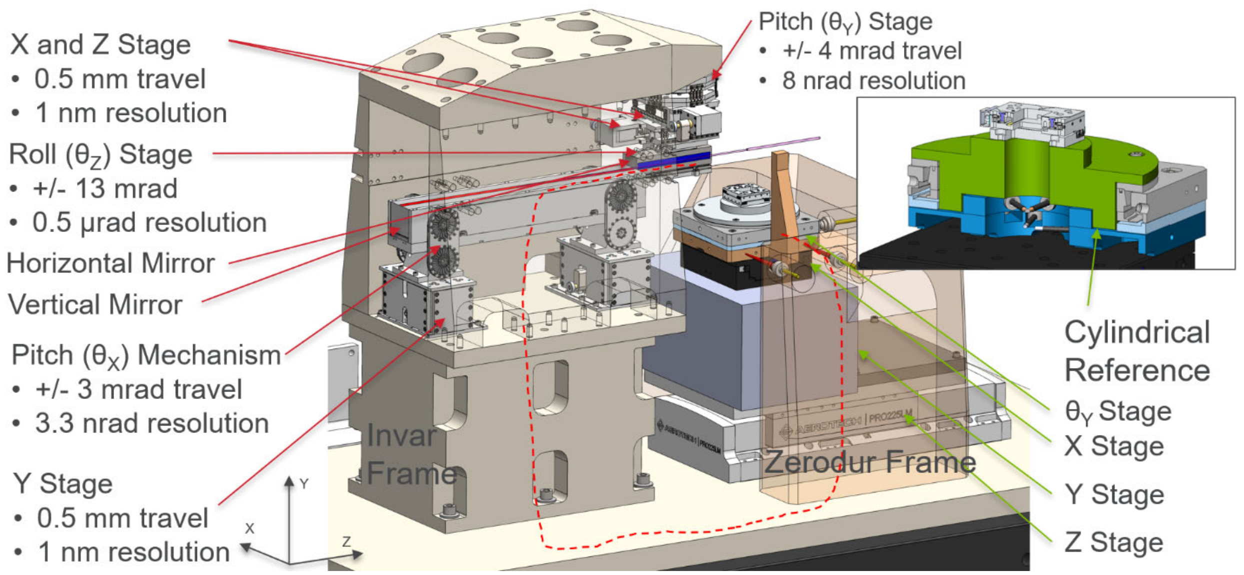

Figure 3: Details of the K-B optics system (left) and sample position stage system (right). The metrology loop is shown as a dashed line, and the inset shows the cylindrical reference mounted to the sample rotation stage.

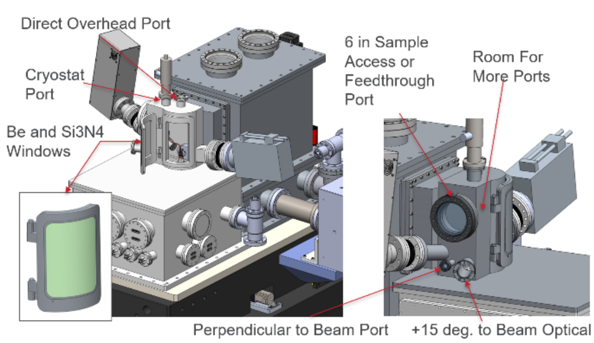

Figure 4: Model showing details of the ports and windows.

K-B System

The K-B optical system is shown in Fig. 3. The mirrors are positioned using nanopositioning flexure stages designed using Shu *et al.* [9] weak-link flexures. The vertical mirror is positioned vertically and pitched by differentially moving the vertical stages. A gantry type geometry is used for the horizontal mirror and stages to provide room for the sample chamber underneath. It is positioned in X, Z, pitch, and roll. More detail on the stages can be found in [10].

Sample Scanning System

A model of the sample scanning system is shown in Fig. 3. It is designed to handle up to a 2 kg load with 1 mm/s scan speed in X and Y over an area of 10 mm x 10 mm. A piezo rotation stage atop the XYZ stack is used for tomography and ptychography imaging. The last stage above the rotation stage is an XZ piezo linear stage to position the sample at the rotation center.

A direct drive stage will be used for scanning in the X direction and is sized so that, even at full speed and 5 Hz oscillation over a 100 µm scan, coil temperatures are expected to rise by 0.06 °C in vacuum. This is with the expectation that any external forces due to wires or tubing lines are negligible. Much care will be taken in the finalizing of the design for strain relieving cables and tubes to provide enough slack for motion but not too much so that the stage is lifting cables.

Metrology

By separating the optics and sample environment the metrology frame to measure the relative position of the sample with respect to the optics becomes complicated. Fig. 3 shows the metrology loop with the vacuum chambers removed for clarity. The measurement loop must travel through 466 mm in the vertical direction down to the common Invar reference base. Then it is assumed that the Invar reference base is moving or deforming evenly across the plate. After the plate it then moves up through a Zerodur frame to the sample level. The Zerodur frame was chosen for the sample side since it does not have to support a load, as in the optics case, and it will be in the region with greatest heat load.

Errors from the rotation stage are corrected after each rotation step. The runout, wobble, and flatness errors are measured by capacitive sensors looking at a diamond turned reference cylinder. The errors will then be fed back to the XYZ stack to correct the errors.

CONCLUSION

The instrument design is close to completion, with procurement of components and system integration beginning in 2022.

ACKNOWLEDGEMENTS

We wish to thank S. Bean, from the APS, Y. Chu, H. Yan, and E. Nazaretski from the Hard X-ray Nanoprobe at the National Synchrotron Light Source II at Brookhaven National Laboratory, and N. Guisinger and J. Wen from Argonne's Center for Nanoscale Materials for help measuring foundation stability.

ISBN: 978-3-95450-229-5 ISSN: 2673-5520 doi:10.18429/JACoW-MEDSI2020-MOPC10

REFERENCES

[1] J. Maser *et al*., "A next-generation hard x-ray nanoprobe beamline for *in situ* studies of energy materials and devices," *Metall. Mater. Trans. A*, vol. 45, no. 1, pp. 85-97, 2014. doi: https://doi.org/10.1007/s11661-013-1901-x

[2] J. Maser *et al*., "Design concept for the *in situ* nanoprobe beamline for the APS upgrade," *Microsc. Microanal.*, vol. 24, suppl. S2, pp. 194-195, 2018. doi:10.1017/S1431927618013314

[3] S. P. Kearney, S. Bean, and J. Maser, "Analysis of vibration isolated facilities for the in situ nanoprobe at the Advanced Photon Source," *Synchrotron Radiat. News*, vol. 32, iss. 5, p. 13, 2019. doi:10.1080/08940886.2019.1654827

[4] https://www.aps.anl.gov/APS-Upgrade

[5] C. Preissner *et al*., "A family of high-stability granite stages for synchrotron applications," presented at the 11th Int. Conf. on Mechanical Engineering Design of Synchrotron Radiation Equipment and Instrumentation (MEDSI2020), Chicago, IL, USA, virtual conference, July 2021, paper THOA01, this conference.

[6] B. M. Das, *Fundamentals of Soil Dynamics*. New York, NY, USA: Elsevier Science Publishing Co., Inc., 1983.

[7] S. P. Kearney *et al*., "A comparison of isolated and monolithic foundation compliance and angular vibrations," *APS/CNM Users Meeting*, Lemont, IL, USA, May 2019, poster abstract, https://www.aps.anl.gov/Users-Information/User-Community/Users-Meetings/Program/Archive/2019/Program-Book

[8] F. Cacho-Nerin, J. E. Parker, P. D. Quinn, "A passive hutch-cooling system for achieving high thermal-stability operation at the nanoprobe beamline, Diamond Light Source," *J. Synchrotron Radiat.*, vol. 27, Supporting information, 2020. doi:10.1107/S1600577520004932

[9] D. Shu *et al*., "Applications of laminar weak-link mechanisms for ultraprecision synchrotron radiation instruments," *AIP Conf. Proc.*, vol. 879, iss. 1, pp. 1073-1076, 2007. https://doi.org/10.1063/1.2436249

[10] D. Shu *et al*., "Modular nanopositioning flexure stages development for APS upgrade K-B mirror nanofocusing optics," presented at the 11th Int. Conf. on Mechanical Engineering Design of Synchrotron Radiation Equipment and Instrumentation (MEDSI2020), Chicago, IL, USA, virtual conference, July 2021, paper TUPC10, this conference.